



# Optical absorber based on self-similar cylindrical element for detecting optical material

Sepideh Ebrahimi<sup>1</sup>

Received: 15 August 2019 / Accepted: 22 January 2020 / Published online: 29 January 2020  
© Springer Science+Business Media, LLC, part of Springer Nature 2020

## Abstract

In this paper, an optical absorber based is exploited on self-similar cylindrical for material detection in the infrared spectrum as a refractive index sensor. Two models are suggested and the effect of the gaps is discussed. Actually, the gaps can be used for intensifying the absorption and improving the figure of merit (FOM). The absorber is modified for 300 THz (1000 nm) with reflection value of  $-45$  dB (0.004) which is made this absorber as a good choice for optical refractive sensing. This study shows the importance of the parasitic elements and gaps for improving the sensing quality and FOM value. In fact, the reflection of the Nanoabsorber is increased extremely without using the parasitic element up to  $-14$  dB. As shown in this paper, the FOM of the prototype absorber is enhanced more than 10 times for some refractive indexes by implementing of gaps. The maximum value of the FOM is  $400 \text{ RIU}^{-1}$  for the final model with gap and the maximum sensitivity is  $204 \text{ nm/RIU}$  obtained for the structure without the gap. In brief, these gaps can be considered for increasing the FOM more than the basic model.

**Keywords** Absorber · Self-similar · FOM · Infrared · Refractive index sensing

## 1 Introduction

Identification of materials at different operation frequencies is important. Therefore, various sensors have been designed for medical sensing (Pignalosa et al. 2012) at terahertz (Azizi et al. 2018) and in the optical spectrum (Cetin et al. 2015). Of course, nanoscale sensors should be designed to identify very small molecular quantities such as organic materials (Kvasnička et al. 2012). Therefore, devices such as nano-antennas (Zarrabi et al. 2017) and nano-absorbers (Nouri-Novin et al. 2019) are mainly considered.

On the other hand, with the advancement of physics, the plasmonic concept could be understood clearly by researchers (Deng et al. 2019). This is based on the collision and interaction of light with metal and gathering surface plasmon at the interface of metal and dielectric (Kim et al. 2016). This feature is intended to strengthen the field and design of compact devices (de Ceglia et al. 2015).

---

✉ Sepideh Ebrahimi  
sepideh.ebrahimi87@yahoo.com

<sup>1</sup> Department of Engineering, Islamic Azad University, Aligoudarz Branch, Aligoudarz, Iran

For this purpose, various structures have been proposed to improve the absorption and minimization of structures (Soheilifar and Zarrabi 2019; Soheilifar 2018). The first category is planar structures with simple elements, such as disks (Liu et al. 2010). The second is the planar structures with complex metamaterial forms (Tavakoli et al. 2019). In this structure, gaps play an important role in enhancing absorption (Bazgir et al. 2018). The third category is volumetric structures that are made up of a three-dimensional shape (Xu et al. 2016).

The use of absorbers is not only limited to medical devices (Wu et al. 2012) and the detection of materials, but also for solar cells (Jain et al. 2016) and renewable energy production. However, for designing the absorber as a sensor, the various concepts such as sensitivity and figure of merit (FOM) have been used for determining the quality of a sensor (Cheng et al. 2016; Zheng et al. 2017). Usually, the optical waveguide is well-known for refractive index sensing because of high FOM value with Fano response (Zhang and Cui 2019), but fabrication and implementation of these sensors for spectroscopy are too hard, therefore the absorbers are more interesting for surface enhancement and concentrating of energy despite their low FOM value (Le 2018; Meng et al. 2017).

Recently, fractal and self-similar structures are used for the design of absorbers (Rodrigo et al. 2018). As a matter of fact, the reason for the use of these structures is to reduce the polarization dependence in these absorbers (Ishikawa and Tanaka 2015; Meng et al. 2019). Cross-shaped structures are commonly used in the design of absorbers because of the easy design and the polarization independency (Tavakoli et al. 2019; Heydari et al. 2017).

Accordingly, we proposed a self-similar structure based on cylindrical with cross formation, with four parasitic elements on the four corners. In this paper, we will examine the effect of these parasitic elements and compare polarization independency using a parasitic elemental structure with parasitic elements model. Finally, the effect of gaps and height to improve reflection is studied. In the end, we will find the sensitivity and FOM for the proposed structure and compare each other.

## 2 Absorber design and modelling

The electromagnetic behavior of metals is expressed in various frequencies based on their permittivity  $\varepsilon(\omega)$  (Giannini et al. 2011). On the other hand, the description of the electromagnetic behavior of metals by using the free electron gas model at optical frequencies is invalid, due to the effect of the integrand transition. This effect can be considered using the Lorentz–Drude model, so that the permittivity is as follows (Tavakoli and Ebrahimi 2019):

$$\varepsilon(\omega) = 1 - \frac{\omega_p^2}{\omega^2 + \gamma^2} \quad (1)$$

where  $\varepsilon_\infty$  is the relative permittivity at the infinite frequency and  $\omega_p$  is the Plasma frequency of the free electron gas model, the resonant frequency ( $\omega_0$ ) will be zero, and  $\gamma_0$  is the collision frequency (Tavakoli and Ebrahimi 2019). Here, we have used the gold for the metal section with  $\varepsilon_\infty = 9.1$ ,  $\omega_p = 1.38 \times 10^{16}$  Hz and  $\tau = 9.3 \times 10^{-15}$  ( $\tau = 1/\lambda$ ).

Figure 1 shows the proposed structure for the perfect absorber, which is a metal-isolator-metal (MIM) structure. And the underlying layer is an integrated gold layer based on the Drude model, which has been created in CST as described in the previous section. The Isolator or spacer layer is a dielectric, which we have used the silicon with a refractive

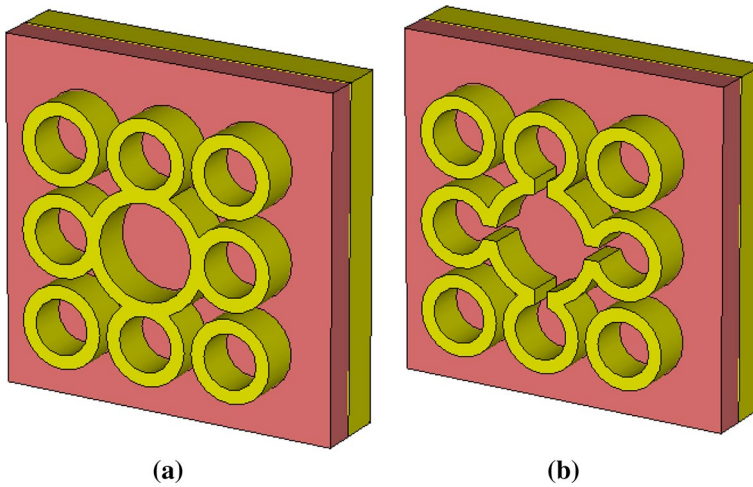


**Fig. 1** The prototype absorber based on cross formation with parasitic elements **a** without gap, **b** with gap

index of 3.24. Finally, the upper layer is again gold with a height of 60 nm, which is actually a number of cylinders with an inner radius of 40 and an outer of 60 nm. As shown in Fig. 1, our absorber structure consists of 9 cylinders arranged in a  $3 \times 3$  formation. But the central cylinder has the inner radius of 90 nm and the outer radius 70 nm which is larger than the other cylinders to form the cross structure as shown in Fig. 1a. Then, some gaps are added to the cross structure, as seen in Fig. 1b, that increase the energy concentration and thus improve the quality of the sensor and the reflection value.

Here, we have used CST Microwave Studio for modelling the prototype absorber based on the Time-domain simulation with perfect match layer (PML). The periodic boundary conditions are used for walls in X and Y directions while the open and space are utilized for Z- direction and wave-ports are placed in +Z and -Z for two ports analyses. We extract  $S_{11}$  and  $S_{21}$  form simulation, where  $R(\omega) = |S_{11}|^2$ ,  $T(\omega) = |S_{21}|^2$  and  $A(\omega) = 1 - |S_{11}|^2 - |S_{21}|^2$  are the reflectance, transmission and absorbance respectively (Soheilifar 2019).

### 3 Simulation result and discussions

Here we examine the reflection and absorption of the two proposed models which are presented in Fig. 1 and the results are presented and compared in Fig. 2. Figure 2a shows the reflection value for the two structures. As shown here, the absorption value for the second model when we used the gaps in the structure, the reflection is decreased to  $-45$  dB, with an operating frequency of 300 THz (1000 nm). On the other hand, for the structure without gap, the reflection is about  $-24$  dB and at 310 THz (967 nm). In short, using the gap can be increased energy and absorption, which are very important for the surface-enhanced infrared absorption spectroscopy (SEIRA) (Durmaz et al. 2018) method to identify biological materials. As shown in Fig. 2b, the first model's absorption is about 91% while the absorption of the final model is obtained more than 99.9%. So we can assume it as a perfect absorber. In fact, we obtain the reflection value of 0.004 for the final model which is considerable for achieving the high FOM value for material detecting.

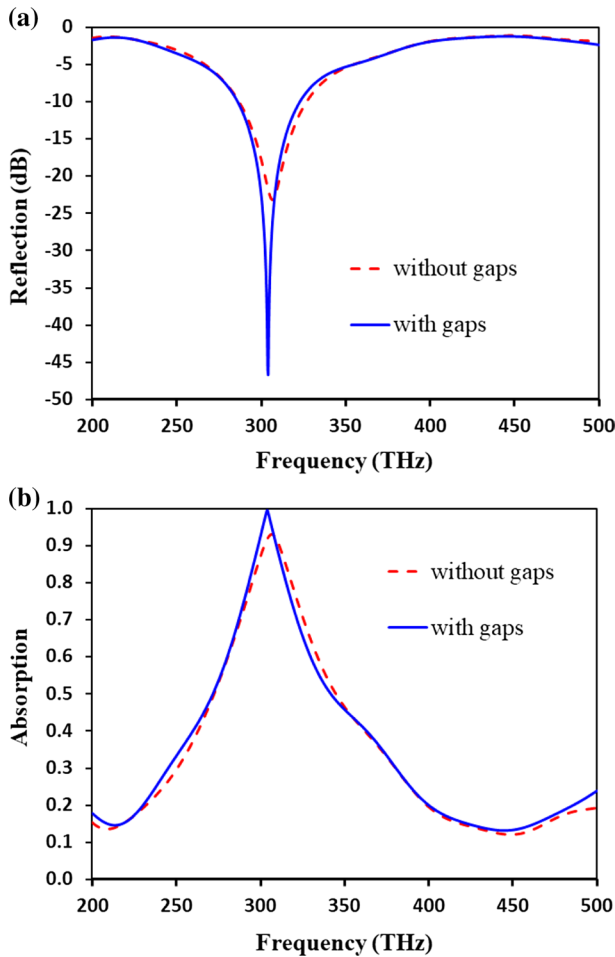


**Fig. 2** The reflection and absorption of the proposed absorber **a** reflection, **b** absorption

We have checked the parasitic element effect on the reflection of both models and the results underscore in Fig. 3. By comparison between Figs. 3 and 2a, we can realize the importance of parasitic element for enhancing the reflection and absorption. In the absence of the parasitic element, the reflection value of both models is reduced drastically while for the first model the reflection is reduced from  $-24$  to  $-21$  dB. On the other hand, the variation of reflection value for the second model in the absence of the parasitic element is more egregious while it reduced from  $-45$  to  $-14$  dB. Therefore, it means the reflection value increase from 0.004 to 0.25 which is not interesting for designing a sensor with high FOM value. To sum up, we can say that the reflection value can be modified by two factors of the gap and parasitic element in this type of absorber.

The electrical field is compared for both suggested model in Fig. 4 for 300 THz (1000 nm). As shown in Fig. 4, the electric inclines to dispense in dipole mode and formation in Y-direction. However, the parasitic elements change the electric field distribution in the omnidirectional pattern. Moreover, the gaps play an important role in making

**Fig. 3** The reflection of the both model in absence of parasitic elements

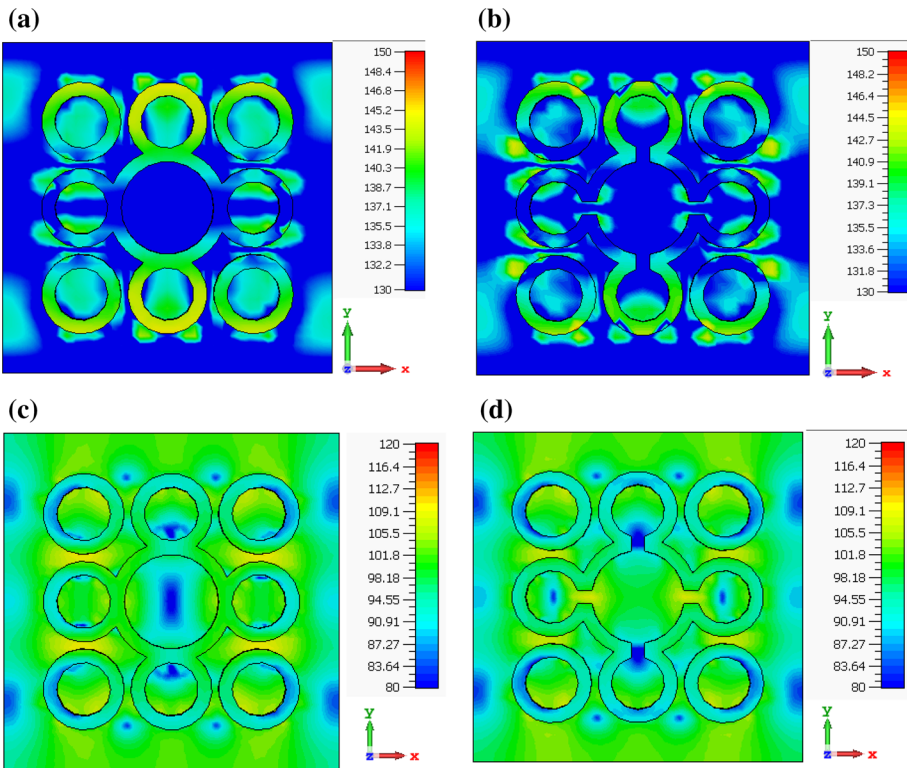
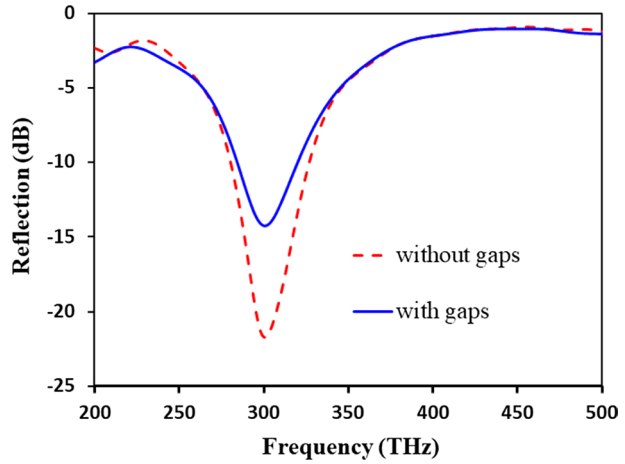


**Fig. 4** The for both suggested models at 300 THz **a** E-field for the structure without gaps, **b** E-field for the structure with gaps, **c** H-field for the structure without gaps, **d** H-field for the structure with gaps

new sections for energy saving. As shown in Fig. 4b the gaps are important for controlling the electric field distribution in the main object and parasitic elements. The H-field for the structure without gaps is presented in Fig. 4c as shown here, the fields are dispensed

between the parasitic element and main element and when the gaps are implemented, the field is concentrated in this gap too as shown in Fig. 4d.

## 4 The parametric study of the absorber

Various parameters usually impact on reflection and absorption of an absorber. However, some of them are not important, but some factors have monumental effect which should be studied for analyzing the behavior of an absorber. Here, we have selected a few important parameters such as the height of the elements and gaps width.

### 4.1 The height of the elements effect

The height of the elements is important for absorber because its effect on the amount of surface plasmon polariton (Cheng et al. 2018) and in addition, the gaps are playing an important role for controlling the resonance because the gaps are making capacitance and the length of the cylindrical element plays the role of inductance (Cheng et al. 2018). In Fig. 5, variations of reflectance are shown for different values of nanoparticle's height. As shown in Fig. 5, with the increase in the height of the reflection, thus the absorbance and FOM extremely improved. For a height of 20 nm, the reflection is  $-13$  dB, but reaches  $-45$  dB for a height of 60 nm. We should notice that the height variation doesn't have any shift in frequency while we have assumed the size of the gaps 20 nm.

### 4.2 The gap's width effect

The gaps are another important factor for controlling the reflection and resonances (Zarrabi et al. 2018). Here, we have checked the reflection of the final absorber for gaps between 10 and 40 nm and results are presented in Fig. 6. As shown in this study, the reflection value relation with gaps has nonlinear behavior and gaps dimension hasn't any essential effect on the frequency resonance, but by increasing the gaps' size from 10 to 20 nm, the absorber reflection is drastically reduced.

**Fig. 5** The reflection of the structure with gap for various heights

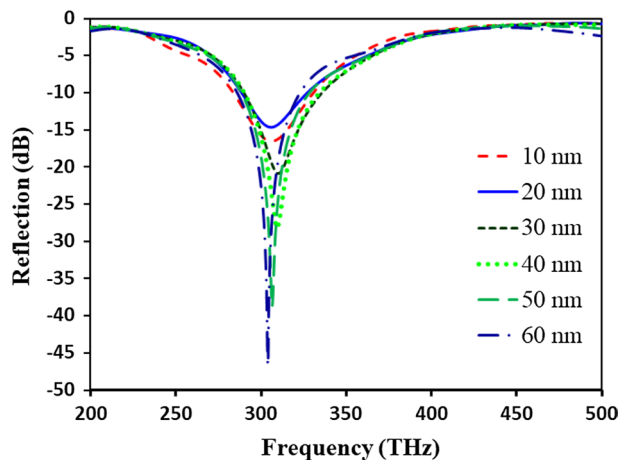
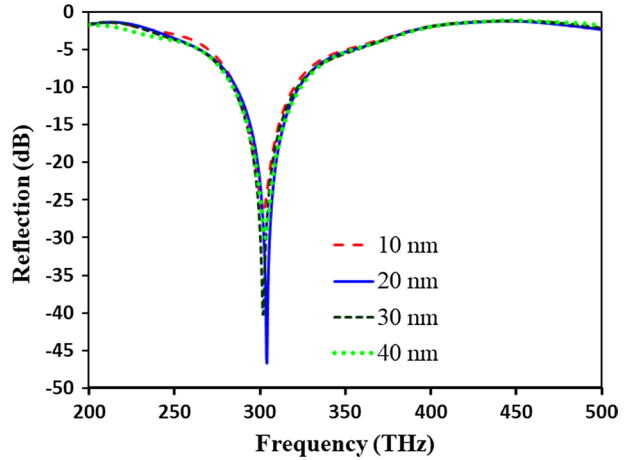


**Fig. 6** The reflection of the structure with gap for various heights



## 5 Refractive index sensing by absorber

In order to evaluate the performance of the sensors, some parameters such as sensitivity ( $S$ ) and merit criterion (FOM) are evaluated. The change in the output for change is defined as the size of a unit of interest for measurement. The sensitivity of the refractive index is the sensitivity of the SPR sensor to the refractive index ( $n$ ) and by changing the refractive index  $\Delta n$  of the environment around the sensor, the resonance wavelength varies  $S = \Delta\lambda / \Delta n$ . In some cases, sensitivity is not used alone. So that if there is a coating on a substrate, the frequency response changes. Therefore, by examining the extent of changes such as frequency shifts, we can extract the proportion that this ratio can be based on different concepts. For clarity to be considered, the FOM parameter is  $FOM = S / FWHM$  defined as FWHM the maximum bandwidth of the resonance spectrum at half the maximum power. In some cases, the FOM parameter is defined as  $FOM = \max[\Delta R / (R \times \Delta n)]$  that  $R$  reflectance value is in resonance, and  $\Delta R$  the reflectance variations due to small changes are the refractive index  $\Delta n$  (Zheng et al. 2017; Bazgir et al. 2020).

In order to test the sensitivity and FOM parameters, we covered the absorber surface with the material under-test with a height of 100 nm and provided frequency variations for various refractive indexes.

Here, we consider the variation of the refractive index from 1 to 1.2 with steps of 0.05 and check for both structures without gap and with gap and the results for these two modes are presented in Fig. 7.

As shown in Fig. 7a, b, the resonances shifted to lower frequency by increasing the refractive index value and this is due to the change in the capacitive properties of the structure. In addition, the reflection value is reduced typically where the reflection decreased from  $-47$  dB for  $n=1$  at 310 THz (967 nm) to  $-33$  dB for  $n=1.2$  at 290 THz (1033 nm) for the second structure.

In Fig. 8, we have examined two fundamental parameters of FOM and sensitivity for two different structures. As shown in Fig. 8a, the sensitivity of the structure without the gap is twice the proposed structure with the gap. In fact, the gap increases the Q-factor and reduces the impact of materials on the external capacitor for the test substance. Here, the maximum sensitivity for  $n=1.05$  for the first structure is 204 nm/RIU, and for the final structure that creates the gap, it is 100 nm/RIU.

**Fig. 7** The reflection of the both model for various refractive index **a** the structure without gaps, **b** the structure with gaps

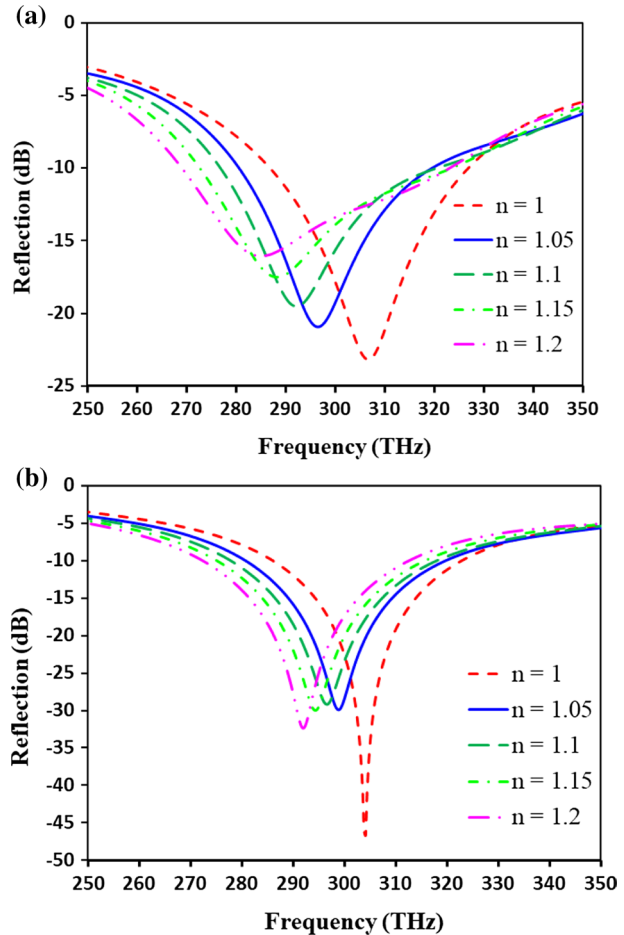


Figure 8b shows the FOM variations in terms of refractive index. As shown in the Fig. 6, the FOM has greatly increased for the structure with a gap in comparison with the previous structure. In fact, FOM has increased from 34 to 396  $\text{RIU}^{-1}$ , for  $\Delta n=0.05$ . In addition, for  $\Delta n=0.15$ , the value of FOM has increased from 16 to 203  $\text{RIU}^{-1}$ . So, the FOM has increased more than 10 times when we have used the gaps with the width of 20 nm.

In fact, the gaps make capacitances which help us to save more energy in the structure and so, the reflection reduces drastically and the material under test makes another capacitance around the absorber and by increasing the refractive index the loss and effect of this capacitance will increase and reduce the FOM and sensitivity.

## 6 Comparison with other research

Nowadays various models of optical absorber have been developed for refractive index sensing and for this goal 3D structure is known as more effective devices because of higher reflection which is an important value for obtaining better FOM value. In Table 1, the



**Fig. 8** The sensor parameter for prototype absorber **a** the sensitivity for absorber with and without gaps, **b** the FOM for absorber with and without gaps

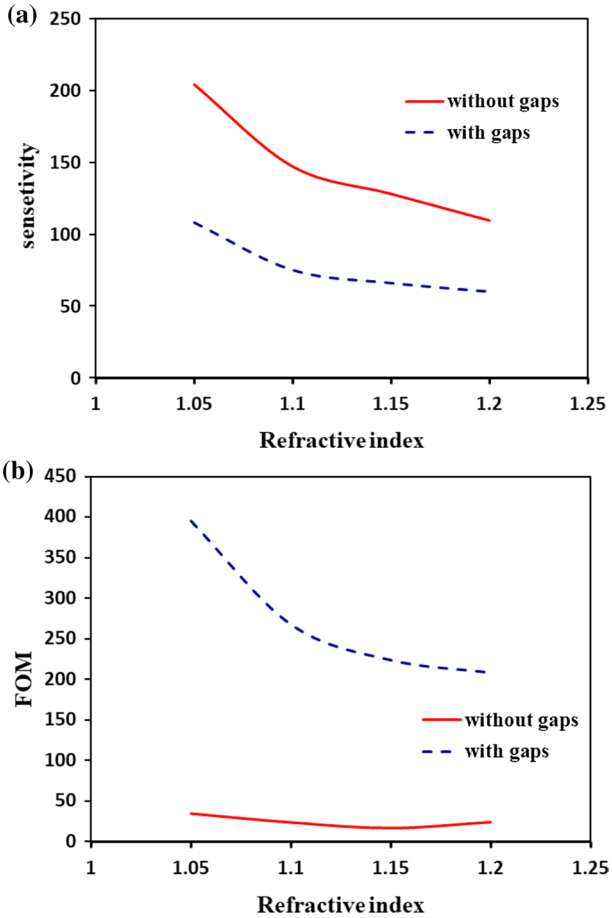


**Table 1** The comparison of the absorber prototype with previous works

References	Minimum reflection (dB)	Bandwidth (%)	Sensitivity (nm/RIU)	FOM (RIU <sup>-1</sup> )	Frequency/wavelength
This work	-47	12.8	204	400	285–324 THz (925–1051 nm)
Nouri-Novin et al. (2019)	-12	3	52.5	-	164–169 THz (1773–1828 nm)
Soheilifar and Zarrabi (2019)	-30	3.5	-	-	94–97 THz (3090–3189 nm)
Soheilifar (2018)	-47	25	-	10,600	190–245 THz (1223–1577 nm)
Tavakoli et al. (2019)	-50	3	473	2424	330–340 THz (890–900 nm)
Soheilifar (2019)	-18	21	-	1856	172–210 THz (1427–1742 nm)

comparison of prototype absorber with the previous model is presented. We compare bandwidth, minimum reflection and frequency range of the prototype and other models. The minimum value of reflection is obtained  $-47$  dB which more than other previous models and however, in (Soheilifar 2018) was reported  $-47$  dB for lower frequency and it is hard to modify the absorber at a higher frequency. In (Soheilifar 2018) and (Soheilifar 2019) have been reported the bandwidth of 25 and 21% respectively but other absorbers have lower bandwidth such taper rectangular element in (Nouri-Novin et al. 2019). In this paper, the bandwidth is about 12.8% which makes this absorber attractive for other application such as solar cell.

## 7 Conclusion

Different methods have been considered to improve the absorption of plasmonic absorbers, which we used two kinds of them in this study. These two methods are the using of the parasitic element and creating a gap in the structure. Here, we show how much these two methods have a positive effect on the absorption and sensor properties such as FOM. We have been able to improve the FOM to  $400 \text{ RIU}^{-1}$  and improving the average FOM by 10 times only by using of gaps. We obtained reflection value of  $-47$  dB and bandwidth of 12.8% for this type of absorber.

## References

- Azizi, S., Nouri-Novin, S., Seyedsharbaty, M.M., Zarrabi, F.B.: Early skin cancer detection sensor based on photonic band gap and graphene load at terahertz regime. *Opt. Quant. Electron.* **50**(6), 230 (2018)
- Bazgir, M., Novin, S.N., Zarrabi, F.B., Heydari, S., Arezoomand, A.S.: A novel plasmonic elliptical nanocluster and investigating Fano response in  $\pi$ - and T-shaped arrays. *Electromagnetics* **38**(4), 207–216 (2018)
- Bazgir, M., Jalalpour, M., Zarrabi, F.B., Arezoomand, A.S.: Design of an optical switch and sensor based on a MIM coupled waveguide using a DNA composite. *J. Electron. Mater.* 1–6 (2020)
- Cetin, A.E., Turkmen, M., Aksu, S., Etezadi, D., Altug, H.: Multi-resonant compact nanoaperture with accessible large nearfields. *Appl. Phys. B* **118**(1), 29–38 (2015)
- Cheng, Y., Mao, X.S., Wu, C., Wu, L., Gong, R.Z.: Infrared non-planar plasmonic perfect absorber for enhanced sensitive refractive index sensing. *Opt. Mater.* **53**, 195–200 (2016)
- Cheng, Y., Zhang, H., Mao, X.S., Gong, R.Z.: Dual-band plasmonic perfect absorber based on all-metal nanostructure for refractive index sensing application. *Mater. Lett.* **219**, 123–126 (2018)
- de Ceglia, D., Vincenti, M.A., De Angelis, C., Locatelli, A., Haus, J.W., Scalora, M.: Role of antenna modes and field enhancement in second harmonic generation from dipole nanoantennas. *Opt. Express* **23**(2), 1715–1729 (2015)
- Deng, X., Li, L., Enomoto, M., Kawano, Y.: Continuously frequency-tuneable plasmonic structures for terahertz bio-sensing and spectroscopy. *Sci. Rep.* **9**(1), 3498 (2019)
- Durmaz, H., Li, Y., Cetin, A.E.: A multiple-band perfect absorber for SEIRA applications. *Sens. Actuators B Chem.* **275**, 174–179 (2018)
- Giannini, V., Fernández-Domínguez, A.I., Heck, S.C., Maier, S.A.: Plasmonic nanoantennas: fundamentals and their use in controlling the radiative properties of nanoemitters. *Chem. Rev.* **111**(6), 3888–3912 (2011)
- Heydari, S., Bazgir, M., Zarrabi, F.B., Gandji, N.P., Rastan, I.: Novel optical polarizer design based on metasurface nano aperture for biological sensing in mid-infrared regime. *Opt. Quant. Electron.* **49**(2), 83 (2017)
- Ishikawa, A., Tanaka, T.: Metamaterial absorbers for infrared detection of molecular self-assembled monolayers. *Sci. Rep.* **5**, 12570 (2015)

- Jain, P., Shokeen, P., Arun, P.: Improved efficiency of plasmonic tin sulfide solar cells. *J. Mater. Sci.: Mater. Electron.* **27**(5), 5107–5113 (2016)
- Kim, J., Kim, S., Nguyen, T.T., Lee, R., Li, T., Yun, C., Ham, Y., An, S.S.A., Ju, H.: Label-free quantitative immunoassay of fibrinogen in alzheimer disease patient plasma using fiber optical surface plasmon resonance. *J. Electron. Mater.* **45**(5), 2354–2360 (2016)
- Kvasnička, P., Chadt, K., Vala, M., Bocková, M., Homola, J.: Toward single-molecule detection with sensors based on propagating surface plasmons. *Opt. Lett.* **37**(2), 163–165 (2012)
- Le, K.Q.: Enhanced circular dichroism via symmetry breaking in a chiral plasmonic nanoparticle oligomer. *J. Electron. Mater.* **47**(5), 2836–2840 (2018)
- Liu, N., Mesch, M., Weiss, T., Hentschel, M., Giessen, H.: Infrared perfect absorber and its application as plasmonic sensor. *Nano Lett.* **10**(7), 2342–2348 (2010)
- Meng, H., Wang, L., Liu, G., Xue, X., Lin, Q., Zhai, X.: Tunable graphene-based plasmonic multispectral and narrowband perfect metamaterial absorbers at the mid-infrared region. *Appl. Opt.* **56**(21), 6022–6027 (2017)
- Meng, W.W., Lv, J., Zhang, L., Que, L., Zhou, Y., Jiang, Y.: An ultra-broadband and polarization-independent metamaterial absorber with bandwidth of 3.7 THz. *Opt. Commun.* **431**, 255–260 (2019)
- Nouri-Novin, S., Sadatgol, M., Zarrabi, F.B., Bazgir, M.: A hollow rectangular plasmonic absorber for nano biosensing applications. *Optik* **176**, 14–23 (2019)
- Pignalosa, P., Liu, B., Chen, H., Smith, H., Yi, Y.: Giant light extraction enhancement of medical imaging scintillation materials using biologically inspired integrated nanostructures. *Opt. Lett.* **37**(14), 2808–2810 (2012)
- Rodrigo, D., Tittl, A., John-Herpin, A., Limaj, O., Altug, H.: Self-similar multiresonant nanoantenna arrays for sensing from near-to mid-infrared. *ACS Photonics* **5**(12), 4903–4911 (2018)
- Soheilifar, M.R.: Wideband optical absorber based on plasmonic metamaterial cross structure. *Opt. Quant. Electron.* **50**(12), 442 (2018)
- Soheilifar, M.R.: The wideband optical absorber based on plasmonic metamaterials for optical sensing. *Optik* **182**, 702–711 (2019)
- Soheilifar, M.R., Zarrabi, F.B.: Reconfigurable metamaterial absorber as an optical switch based on organic-graphene control. *Opt. Quant. Electron.* **51**(5), 155 (2019)
- Tavakoli, F., Ebrahimi, S.: Planar optical waveguide for refractive index determining with high sensitivity and dual-band characteristic for Nano-sensor application. *Opt. Quant. Electron.* **51**(6), 185 (2019)
- Tavakoli, F., Zarrabi, F.B., Saghaei, H.: Modeling and analysis of high-sensitivity refractive index sensors based on plasmonic absorbers with Fano response in the near-infrared spectral region. *Appl. Opt.* **58**(20), 5404–5414 (2019)
- Wu, C., Khanikaev, A.B., Adato, R., Arju, N., Yanik, A.A., Altug, H., Shvets, G.: Fano-resonant asymmetric metamaterials for ultrasensitive spectroscopy and identification of molecular monolayers. *Nat. Mater.* **11**(1), 69–75 (2012)
- Xu, J., Zhao, Z., Yu, H., Yang, L., Gou, P., Cao, J., Zou, Y., et al.: Design of triple-band metamaterial absorbers with refractive index sensitivity at infrared frequencies. *Opt. Express* **24**(22), 25742–25751 (2016)
- Zarrabi, F.B., Bazgir, M., Ebrahimi, S., Arezoomand, A.S.: Fano resonance for UI nano-array independent to the polarization providing bio-sensing applications. *J. Electromagn. Waves Appl.* **31**(14), 1444–1452 (2017)
- Zarrabi, F.B., Hekmati, R., Bazgir, M., Ebrahimi, S.: Nanoparticle using parallel split rings and implementation of chain for creating Fano resonance with polarization independence for energy harvesting in mid-infrared. *Opt. Quant. Electron.* **50**(12), 452 (2018)
- Zhang, Y., Cui, M.: Refractive index sensor based on the symmetric MIM waveguide structure. *J. Electron. Mater.* **48**(2), 1005–1010 (2019)
- Zheng, G., Zou, X., Chen, Y., Xu, L., Rao, W.: Fano resonance in graphene-MoS<sub>2</sub> heterostructure-based surface plasmon resonance biosensor and its potential applications. *Opt. Mater.* **66**, 171–178 (2017)